4D Affine Registration Models for Respiratory-Gated PET

GJ Klein, BW Reutter, and RH Huesman
Center for Functional Imaging,
Lawrence Berkeley National Laboratory, Berkeley, CA 94720

Abstract

The heart position shifts considerably due to motion associated with the respiratory cycle, and this motion can degrade the image quality of cardiac-gated PET studies. One method to combat this motion-induced blur is a respiratory-gated acquisition followed by recombination of registered image volumes using a rigid-body motion assumption; however, non-rigid deformation of the heart from respiratory motion may reduce the effectiveness of this procedure.

We have investigated a 12-parameter global affine motion model for registration of different respiratory gates in an end-diastolic cardiac PET sequence. To obtain robust estimates of motion, a 4D registration model was devised that encouraged smoothly varying motion between adjacent respiratory time frames. Registration parameters were iteratively calculated using a cost function that combined a least squares voxel difference measure with a penalty obtained from a prediction prior. The prior was calculated from adjacent time frames assuming constant velocity and an affine model. After registration, the principal extension ratios were calculated to measure the degree of non-rigid motion. In data from ten subjects, extension ratios of over 5% were common, indicating that an affine model may provide better registrations and in turn, better motion-corrected composite volumes than could a technique restricted to the 6-parameter rigid body assumption.

I. INTRODUCTION

Cardiac motion due to the respiratory cycle has now been noted by a number of researchers [1, 2]. For techniques like positron emission tomography (PET), which require much longer than a single breath hold to acquire, this motion can degrade the image quality of cardiac-gated studies. Respiratory-gated acquisition followed by recombination of registered image volumes is one method of combating this motion-induced blur. Our prior efforts in respiratory motion compensation have assumed a rigid-body motion model while registering the image data [3]. Though the respiratory motion can be primarily described as a rotation and translation, it is known that this model is an approximation, since the heart deforms somewhat as it is being pushed and pulled by the diaphragm and other connected tissue. For example, measurements on dogs using high resolution gated CT showed that total heart volume changed by an average of 12% during inspiration, a fact that can only be explained by a non-rigid deformation [4]. Similar shape changes have been found in human subjects using echocardiography [5]. This deformation of the heart from respiratory motion may reduce the effectiveness of a motion compensation procedure that assumes only rigid motion.

We have investigated a 12-parameter global affine motion model for registration of different respiratory gates from a doubly gated cardiac PET sequence. In addition to the six parameters of rotation and translation, the affine model allows for three scale and three skew parameters. To obtain more robust estimates of motion from a sequence of noisy images, a four-dimensional (4D) registration model was devised that encouraged smoothly varying motion between adjacent time frames. Registration parameters were iteratively calculated using a least squares voxel difference cost function combined with a penalty from a prediction affine motion model. The prediction model was computed assuming constant motion velocity between frames. After registration, principal extension ratios were calculated to indicate the extent of non-rigid motion. In the data from ten subjects, stretch ratios of over 5% were common, indicating that the rigid body motion model may contribute to artifacts when combining registered datasets. Using these stretch ratios, a cardiac phantom was used to investigate the impact of improperly aligning a non-rigidly deforming body with a rigid-body motion model.

II. METHODS

A. Data Acquisition

List mode cardiac PET data were acquired from ten subjects using the CTI/Siemens ECAT EXACT HR scanner. Data were acquired from ^{18}F-fluorodeoxyglucose emission studies after the isotope had cleared the blood pool. The data were retrospectively gated for both the respiratory and cardiac cycle to obtain a 2D array of reconstructed volumes. One axis of the array represented the heart at eight different respiratory positions; the other axis represented two different phases of the cardiac cycle.

Monitoring of the respiratory cycle was carried out by taking short, 10-msec time segments of the emission list mode data stream and computing the superior-inferior component of the sinogram center of mass (COM). Because the reconstructed activity distributions were relatively stable in time with the heart as the principal feature in these cases, the COM can be used as an indicator of heart motion [6]. This time-varying waveform could therefore be used as a gating signal to divide the list mode stream into different storage locations based on the respiratory position of the heart. Gating levels were selected to arrive at reconstructed volumes with eight approximately equal respiratory motion components along the superior-inferior direction (long axis of the scanner). In gating for cardiac contractile motion, one phase captured approximately the state of end-diastole, based on the time segments between 0-200 msec and 500+ msec with respect to the R-wave. The other cardiac phase captured primarily the heart as it was contracting through systole. Note

that the image volumes analyzed in this work represent *only* the end-diastole portion of the data. Motion compensation of image volumes obtained from different cardiac phases requires a more complex deformable motion model [7], and will not be discussed further in this paper.

B. Registration Technique

Reconstructed image volumes were spatially smoothed and segmented using a simple percentile-based thresholding operation so that the left ventricle was the principal feature in all image volumes. An initial registration transform was obtained between all volumes in the sequence and the reference volume using a 12-parameter affine motion model and a cost function calculating the least squares cost difference between voxels [8]. For all sequences, end-inspiration was chosen as the reference volume.

Because tomograph events are distributed into many different sinograms in a doubly gated study, the resulting reconstructed volumes are often quite noisy due to insufficient statistics. This characteristic makes a registration algorithm based only on two volumes vulnerable to motion estimation errors. Fortunately, in the case of a 4D dataset like these respiratory gates, we can make use of the *a priori* knowledge that the motion from one gate to another is likely to follow a smooth progression. In fact, since the gating signal boundaries were chose such that the COM intervals were approximately equal, we can assume that the motion between adjacent time frames must also be approximately equal. Therefore, we add a smoothness constraint in time as follows.

Numbering the volumes from 0 to 7, and selecting volume 0 as the reference, the total transformation from any one time frame to the reference volume can be expressed as a 4x4 homogeneous coordinate transformation matrix:

$$M_{0,i} = \begin{bmatrix} a_{0i} & b_{0i} & c_{0i} & d_{0i} \\ e_{0i} & f_{0i} & g_{0i} & h_{0i} \\ i_{0i} & j_{0i} & k_{0i} & l_{0i} \\ 0 & 0 & 0 & 1 \end{bmatrix}$$

Because the motion between adjacent time frames must be consistent with the total motion between distant time frames, the total transformation matrices can be viewed as a cascade of incremental transforms:

$$M_{0,j} = M_{0,1} \ldots M_{j-2,j-1} M_{j-1,j} = \prod_{i=0}^{j-1} M_{i,i+1}$$

Assuming constant velocity between frames, $M_{j-1,j} \approx M_{j-2,j-1}$. Therefore, if we already have estimates of the total transformation matrices for time frames *j* and *j-1*, a prediction transformation for frame *j+1* can be obtained by

$$\tilde{M}_{0,j+1} = M_{0,1} \ldots M_{j-1,j} M_{j-1,j} = M_{0,j} M_{j-1,j}$$

where the incremental transformation matrix, $M_{j-1,j}$, can be obtained by

$$M_{j-1,j} = M_{0,j-1}^{-1} M_{0,j}$$

Table 1. Summary of Registration Parameters

ID	Translation (mm)	λ_x	λ_y	λ_z	$\lambda_x \lambda_y \lambda_z$
1	11.90	1.005	0.999	1.057	1.062
2	16.32	1.015	0.993	1.014	1.022
3	12.59	1.025	0.953	1.076	1.051
4	13.95	1.023	1.033	1.040	1.098
5	12.54	1.031	1.044	1.035	1.113
6	6.77	1.006	1.024	1.030	1.061
7	11.97	1.013	1.008	1.063	1.085
8	1.028	0.999	1.003	0.992	0.993
9	25.42	1.246	1.031	1.203	1.546
10	16.39	1.026	1.003	1.063	1.094

To enforce temporal continuity, we add a cost function component that penalizes departures from the prediction matrix. This is expressed formally as the squared Euclidean norm of the prediction and current estimated transformation difference:

$$E_p(\tilde{M}_{0,j+1}, M_{0,j+1}) = W_p \left| \tilde{M}_{0,j+1} - M_{0,j+1} \right|^2$$

where W_p is a constant used to vary the weight of the prediction term with respect to the voxel difference cost term. After the initial estimates of motion are obtained using information from two adjacent volumes, the prediction cost function is included and a 4D iterative estimation procedure begins. The prediction portion of the cost function encourages a smooth progression of motion between respiratory frames, and makes the motion estimation algorithm more robust when used with low-count reconstructed data.

III. RESULTS

A. Registrations of Human Datasets

Once motion parameters have been estimated, an indication of the departure from a rigid-body model required to register the image data may be obtained by examining the principal extension ratios. These indicate the stretching factors that are required along the three principal axes to register each of the volumes to the reference respiratory time frame.

Affine registration parameters were obtained from the data of ten subjects describing the transformation with respect to a reference frame for all respiratory gates. A summary of results for the transformation between the reference (at end-inspiration) and the most distant respiratory frame (at end-expiration) is seen in Table 1. Here are seen the required translation for a point in the center of the registered volume, the principal extension ratios, $(\lambda_x, \lambda_y, \lambda_z)$, and the compression factor, which is the product of the three extension ratios. For an object that moves with a rigid-body motion, all the extension ratios and therefore the compression factor are equal to 1.0. Viewing the numbers in the table, it can be seen that extension ratios of over 5% are typical, and the extension along the superior-inferior direction (λ_z) is usually largest. Conceivably, this could be explained by the downward pulling motion of the diaphragm during inspiration, which would tend to stretch the heart from its end-expiration shape.

The translations and compression factors necessary to register each gate to the reference at end-inspiration for the ten subjects are shown in Figure 1 and Figure 2 respectively. It is seen that translations are often greater than 10 mm, and range from 1 mm to over 20 mm. Because of the COM gating scheme, the distances are approximately linearly related to the respiratory gate. It is seen that the compression factor is roughly proportional to the translation. The left ventricle size is largest at inspiration, and generally becomes smallest at end-expiration. The compression factors here can be fairly large – close to 10% in some cases.

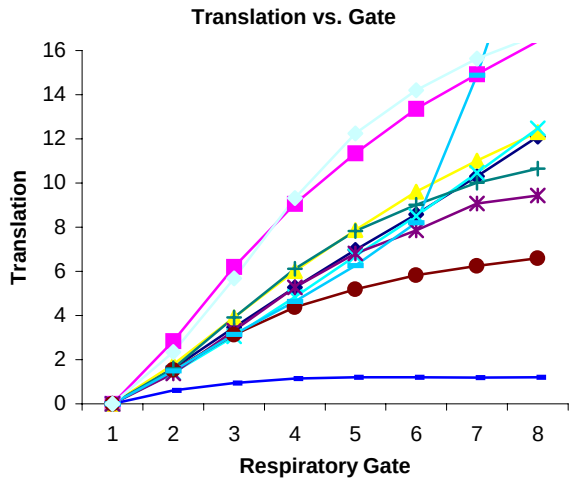

Figure 1. Translation Versus Respiratory Gate. Translations between end-inspiration (gate 1) and end-expiration (gate 8) are typically greater than one centimeter.

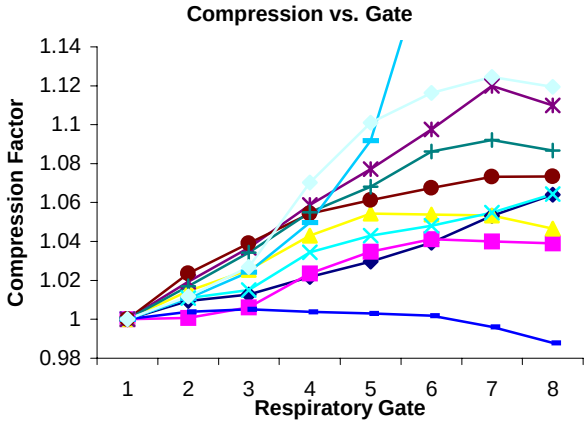

Figure 2. Compression Versus Respiratory Gate. The compression factor is roughly proportional to the translation. The left ventricle appears largest at end-inspiration (gate 1), and smallest at end-expiration (gate 8).

B. Implications of Non-Rigid Respiratory Motion

Given a typical dimension of the left ventricle along the inferior-superior direction of 80-100 mm, a 5% extension ratio would result in a heart image that was 4-5 mm too small if registered using a rigid-body constraint.

When compared to the average 5-10 mm thickness of the left ventricular wall, this scaling error may not be insignificant. This is demonstrated in Figure 3, which shows a transverse view of the ellipsoidal MCAT cardiac phantom [9] and a scaled version that has been stretched by 5%. If one were to try to register these two using a rigid-body motion model, the registration error would be quite large.

Figure 3. Effect of 5% Scaling Difference on Heart Phantom.

Figure 3 points to a worse case example. It shows the maximal extent of misregistration between the most distant respiratory gates for a case with 5% stretch. If we were to add these two volumes together without compensating for the scaling difference, the resulting blur would be considerable. In reality though, a motion compensated composite volume would not be composed of just the two extreme gates, but also of the intermediate gates as well. Furthermore, when imaged with a scanner like the ECAT HR, the peak resolution even in the absence of motion would be limited to 4.1 mm full width at half-maximum (FWHM) transaxially, and 5.4 mm FWHM axially [10], so the additional blur due to scaling errors might not be so problematic.

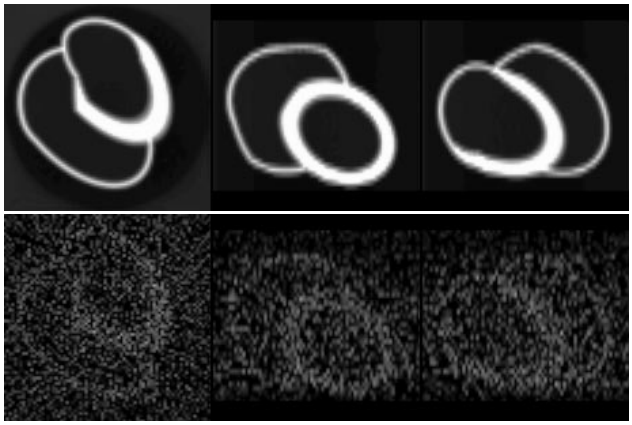

Figure 4. Noisy MCAT Simulation. Noise-free cardiac phantom (top) and noisy version (bottom) are used to test the ability of the 4D algorithm to accurately estimate affine motion parameters. Three orthogonal views (transverse, coronal and sagittal) are shown of each version of the phantom.

To investigate whether an affine motion model would produce noticeably improved motion compensated PET images on a realistic controlled dataset, a noisy version of the MCAT phantom was generated. Starting with a baseline size of the isolated MCAT cardiac phantom on a zero back-

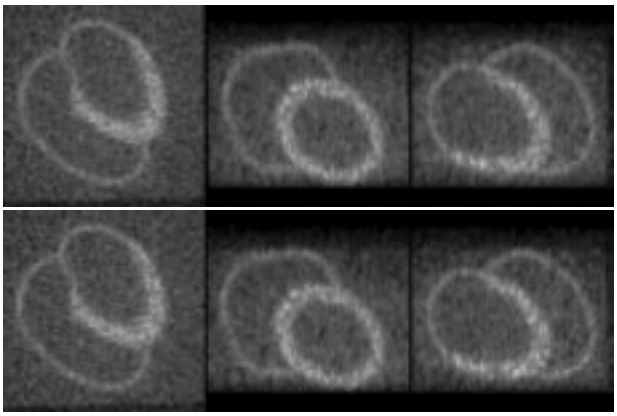

Figure 5. Motion Compensation Comparison. Three orthogonal views of the motion compensated composite cardiac phantom using rigid body model (top), and using the affine model (bottom). Though the actual motion was non-rigid, and 4D affine model was able to estimate it accurately, little difference can be seen in the compensated noisy sums reconstructed at the same spatial resolution of the ECAT HR scanner.

ground, the heart was translated by (1, 7, 13) mm and scaled by stretch factors of (1.05, 1.0, 0.95) in the (x, y, z) directions respectively. Eight equally spaced volumes were created between these two extents. To produce a set of reconstructions with noise characteristics similar to those seen in our human datasets, the eight volumes were first forward projected to obtain a set of noise-free sinograms. Then, these sinograms where sampled using Poisson statistics and reconstructed using filtered backprojection to produce noisy image volumes as seen in Figure 4. Reconstructed voxel size was 2.0x2.0x3.1 mm and sinogram sampling bin size was set the same as the ECAT HR scanner to provide reconstructions with spatial resolution similar to the human datasets.

The reconstructed image volumes were smoothed and segmented, and the 4D affine registrations were estimated as described previously for the human datasets. For comparison, the registrations were also done in two other ways: first by restricting the motion model to only rigid-body motions, and second by allowing affine motions, but not using the 4D smoothing constraint while estimating the motions. The latter method is termed the 3D affine method.

Accuracy of the estimations was judged in two ways: first by the average misregistration distance of seven points dispersed throughout the volume, and second via a qualitative method by comparing the motion compensated composite image volumes. By the first criterion, the accuracy of all three registration methods was quite good. The method restricted to a rigid body model had an average error of 1.32 mm, the 3D affine method had an error of 0.88 mm, and the 4D affine method had an error of 0.78 mm. These results show that even with the amount of noise shown here, fairly accurate registrations could be obtained, and that a 4D affine motion registration method resulted in the least error. In fact, examination of the estimated scale factors for the affine models show that the algorithm was able to estimate the scale factors almost exactly.

The second criterion gives perhaps a more important interpretation of these results. Figure 5 compares the results of motion compensation using the rigid and the affine motion

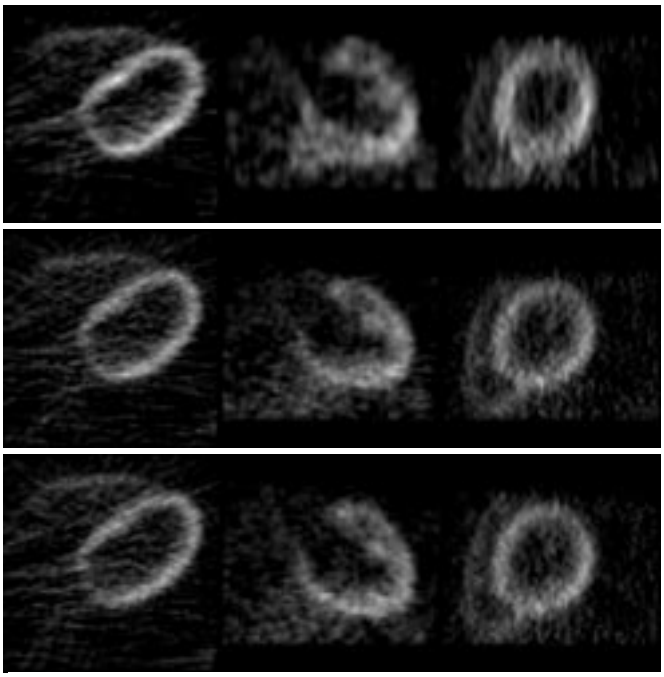

Figure 6. Motion Compensation Comparison on Human PET Data. A direct sum of all respiratory gates without first registering produces a dataset with more blur (top). This is particularly noticeable in the coronal (middle) and sagittal (right) views of the heart. The motion compensated sum using a rigid body motion model (middle) and 4D affine model (bottom) both have improved resolution when compared to the direct sum, however, little advantage can be seen on this dataset by using the 4D affine model.

models. Here, it is seen that even though the affine motion model provided a more accurate registration of all the seven translated and scaled volumes to the reference volume, there is little discernable difference between the best rigid sum (top images) and the best affine sum (bottom images) at this reconstructed spatial resolution.

It is therefore not surprising that similar results are seen when comparing the motion compensation techniques on the human datasets (Figure 6). The top image shows three orthogonal views through the uncompensated images, that is, a simple sum of all gates without first registering the images to the end-inspiration volume. The next two rows show the result of motion compensation. Even though the motion compensated volumes appear to have less blur than the uncompensated sum, there again is little discernable difference between the sum using the rigid-body motion model (middle) and the one using the affine motion model (bottom).

IV. Concluding Remarks

Results presented here can be viewed in two different lights. On one hand, we have shown that the heart does not move purely as a rigid body during the respiratory cycle, and that its motion can better be modeled by an affine motion allowing global scale and skew. On the other hand, we have shown that use of the more accurate affine model to form a composite sum of motion-compensated, registered respiratory gates results in only marginal improvement at the spatial resolution of a conventional whole body PET scanner.

Simulations using a mathematical cardiac phantom have demonstrated that even with very noisy data, accurate estimations of affine motion are possible, and the addition of a 4D smoothness constraint makes the algorithm even more robust. In the images acquired from ten subjects, which were acquired during normal tidal breathing, the heart consistently appeared to compress during expiration. The compression was typically largest along the superior/inferior axis, resulting in a size difference that was often greater than 5%. This suggests that use of a rigid-body motion model to align the two extreme gates of a respiratory-gated cardiac acquisition could result in a registration error comparable to the dimension of the left ventricle wall. Therefore, even though only marginal improvement of motion corrected images is seen in datasets from today's PET scanners, it is likely that as spatial resolution improves, more accurate registration of respiratory gates will assume greater importance.

V. Acknowledgements

The authors would like to thank Thomas Budinger, Elias Botvinick and Nelson Schiller for their helpful discussions, and to Elias Botvinick for his help in providing patient data. This work was supported by NIH grant HL25840 and DOE contract DE-AC03-76SF00098.

VI. References

[1] Y. Wang, S. J. Riederer, and R. L. Ehman, "Respiratory Motion of the Heart: Kinematics and the Implications for the Spatial Resolution in Coronary Imaging," *Magn Reson Med*, vol. 33, pp. 713-719, 1995.

[2] M. M. Ter-Pogossian, S. R. Bergmann, and B. E. Sobel, "Influence of Cardiac and Respiratory Motion on Tomographic Reconstructions of the Heart: Implications for Quantitative Nuclear Cardiology," *J Comput Assist Tomogr*, vol. 6, pp. 1148-1155, 1982.

[3] R. H. Huesman, G. J. Klein, and B. W. Reutter, "Respiratory Compensation in Cardiac PET Using Doubly-Gated Acquisitions," *J Nucl Med*, vol. 38, pp. 114P, 1997.

[4] E. A. Hoffman and E. L. Ritman, "Heart-Lung Interaction: Effect on Regional Lung Air Content and Total Heart Volume," *Ann Biom Engr*, vol. 15, pp. 241-257, 1987.

[5] K. Andersen and H. Vik-Mo, "Effects of Spontaneous Respiration on Left Ventricular Function Assessed by Echocardiography," *Circulation*, vol. 69, pp. 874-879, 1984.

[6] G. J. Klein, B. W. Reutter, and R. H. Huesman, "Data-Driven Respiratory Gating in List Mode Cardiac PET," *J Nucl Med*, vol. 40, pp. 112P, 1999.

[7] G. J. Klein, "Forward Deformation of PET Volumes Using Non-Uniform Elastic Material Constraints," in *Information Processing in Medical Imaging, 16th Annual Conference*, vol. 1613, A. Kuba, Ed.: Springer, 1999, pp. 358-363.

[8] R. P. Woods, S. T. Grafton, J. D. Watson, N. L. Sicotte, and J. C. Mazziotta, "Automated Image Registration: II. Intersubject Validation of Linear and Nonlinear Models," *J Comput Assist Tomogr*, vol. 22, pp. 153-165, 1998.

[9] P. H. Pretorius, W. Xia, M. A. King, B. M. W. Tsui, T. S. Pan, and B. J. Villegas, "Evaluation of Right and Left Ventricular Volume and Ejection Fraction Using a Mathematical Cardiac Torso Phantom," *J Nucl Med*, vol. 38, pp. 1528-1535, 1997.

[10] K. Weinhard, M. Dahlbom, L. Eriksson, C. Michel, T. Bruckbauer, U. Pietrzyk, and W. Heiss, "The ECAT EXACT HR: Performance of a New High Resolution Positron Scanner," *J Comput Assist Tomogr*, vol. 18, pp. 110-118, 1994.